J. Fluid Mech. (2014), *vol.* 743, *pp.* 534–553.
doi:10.1017/jfm.2013.644

Topological selection in stratified fluids: an example from air–water systems

R. Camassa[1], S. Chen[1], G. Falqui[2], G. Ortenzi[2,†] and M. Pedroni[3]

[1]University of North Carolina at Chapel Hill, Carolina Center for Interdisciplinary Applied Mathematics, Department of Mathematics, Chapel Hill, NC 27599, USA

[2]Dipartimento di Matematica e Applicazioni, Università di Milano-Bicocca, Milano, Italy

[3]Dipartimento di Ingegneria, Università di Bergamo, Dalmine (BG), Italy

(Received 24 May 2013; revised 10 October 2013; accepted 3 December 2013; first published online 6 March 2014)

Topologically non-trivial configurations of stratified fluid domains are shown to generate selection mechanisms for conserved quantities. This is illustrated within the special case of a two-fluid system when the density of one of the fluids limits to zero, such as in the case of air and water. An explicit example is provided, demonstrating how the connection properties of the air domain affect total horizontal momentum conservation, despite the apparent translational invariance of the system. The correspondence between this symmetry and the selection process is also studied within the framework of variational principles for stratified ideal fluids.

Key words: channel flow, mathematical foundations, stratified flows

1. Introduction

The determination of conservation laws is an important element of any fundamental understanding of the dynamics of fluids, as well as of any other physical system. The case of the two-dimensional motion of an inviscid, incompressible and heterogeneous fluid is particularly interesting, as it admits an elegant mathematical formulation (Benjamin 1986) and provides a foundation for more complex theories of stratified fluids. Benjamin (1986) introduced a Hamiltonian structure and used it to classify system symmetries and their related conserved quantities. As a side-remark, he pointed out a 'curious' fact: for fluids rigidly confined in (two-dimensional) infinite horizontal-slab domains, horizontal momentum may fail to be conserved, even though it remains a well-defined quantity free of divergences for any localized and bounded initial data.

In Camassa *et al.* (2012, 2013) we isolated and studied this phenomenon, substantiating Benjamin's observation with analytical and numerical results both for one-dimensional long-wave models and for the full two-dimensional Euler equations. In the horizontal slab set-up, with hydrostatic equilibrium conditions at infinity, the violation of momentum conservation is proportional to the difference of the layer-mean pressure at the far ends of the channel. In particular, for the case of two-layer stratification with equal hydrostatic equilibrium at both left and right infinities, this is proportional to the asymptotic interfacial pressure difference

† Email address for correspondence: giovanni.ortenzi@unimib.it

$P_\Delta = P(+\infty) - P(-\infty)$. Explicitly, the time derivative of the total horizontal momentum is

$$\dot{\Pi} = -hP_\Delta, \tag{1.1}$$

h being the height of the slab.

As can be easily shown, P_Δ vanishes in the limit of homogeneous stratification, and, perhaps more remarkably, in the so-called Boussinesq approximation of disregarding density differences in the inertial terms. In Camassa *et al.* (2013), we specifically studied the asymptotic expansion

$$P_\Delta = P_\Delta^{(1)}\rho_\Delta + P_\Delta^{(2)}\rho_\Delta^2 + \cdots,$$

for the small normalized density difference $\rho_\Delta = (\rho_2 - \rho_1)/\rho_2$. In particular, we showed that for vanishing initial velocity the initial pressure difference at $t = 0$ is quadratic in ρ_Δ, i.e. $P_\Delta^{(1)} = 0$ and $P_\Delta^{(2)}$ is the first term in the expansion. Explicit formulae were established at $t = 0$ for this first contribution to the horizontal momentum evolution, particularly for piecewise-constant initial profiles, a set-up that can be – at least in principle – implemented experimentally by use of removable gates.

The focus of the present paper is on a different aspect of the failure of conservation laws in stratified fluids under gravity, one that affects the whole Hamiltonian symmetry structure on which they may be based. When isopycnals intersect boundaries, such as the horizontal plates confining the fluid in a slab domain, these laws may have to be amended or fail altogether, even though configurational symmetries such as invariance under translation may still be present. One of simplest set-ups where this can be seen is that of an air–water system, with water partially filling an infinite horizontal slab between rigid plates, with all fluids in hydrostatic equilibrium at infinity.

We recall that, for air motion with small Mach numbers, air can be considered as incompressible (see e.g. Benjamin 1968; Landau & Lifshitz 1987). This situation can be viewed as the opposite limit of that treated in Camassa *et al.* (2013), since now $\rho_\Delta \to 1$, instead of being small. In what follows, we shall also neglect viscosity and surface tension for both fluids. This assumption can be justified when focusing on configurations and on space–time scales that confine these effects to secondary roles. For instance, viscous effects for a broad class of phenomena enter as boundary layer corrections, leaving the bulk of the fluid free to behave essentially as inviscid. Similarly, surface tension effects can be confined to regions of near-zero spatial measure where typical curvatures are large. In terms of non-dimensional quantities, these assumptions can be expressed concisely by the requirement that the flows we consider have large Reynolds and Bond numbers. (Interestingly, a discussion of the various contributions of surface forces in the context of air–water systems, and within a set-up not unlike the one exemplified here, can be found as early as in the investigations of Bidone (1820). The subdominant role played by surface tension in similar contexts is discussed e.g. in Vanden-Broeck & Keller (1989).)

For simplicity, we assume that our class of motions be invariant along one horizontal direction, y say, thus reducing the slab geometry to one horizontal dimension (a channel) denoted by the x-coordinate. Euler equations for such systems read

$$\rho_j(\boldsymbol{u}_{j_t} + \boldsymbol{u}_j \cdot \nabla \boldsymbol{u}_j) = -\nabla p_j - \rho_j g\, \boldsymbol{k}, \quad \nabla \cdot \boldsymbol{u}_j = 0. \tag{1.2}$$

Hereafter the subscripts $j = a$ and $j = w$ will refer to air and water, respectively, $\boldsymbol{u}_j = (u_j, v_j)$ and ρ_j are the velocities and densities of the two fluids, and $\boldsymbol{k}$ denotes the vertical unit vector for the z-coordinate. Boundary conditions for this system are

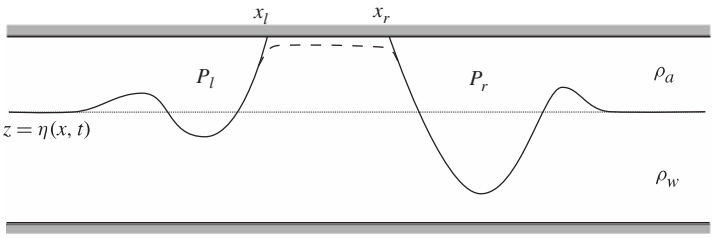

FIGURE 1. Air–water interfaces in an infinite channel, with uniform hydrostatic equilibrium at infinity. The solid line represents a disconnected air domain for which, in general, $P_l \neq P_r$. For the connected case (indicated by the dashed line), in the limit $\rho_a \to 0$ one has $P_l = P_r$ irrespectively of the thickness of the sliver between water and upper plate.

assigned by requiring zero vertical velocities at the rigid plates, while continuity of normal velocity $u_{an} = u_{wn}$ and pressure $p_a = p_w \equiv P$ is imposed at the interface between the two fluids (consistently with our assumption of negligible surface tension). We also assume localized initial data, so that $\boldsymbol{u}_j \to 0$ and the water surface approaches a constant asymptotic level as $|x| \to \infty$ sufficiently fast.

By further ignoring the air mass, the governing equations simplify to

$$\nabla p_a = 0, \quad \rho_w(\boldsymbol{u}_{wt} + \boldsymbol{u}_w \cdot \nabla \boldsymbol{u}_w) = -\nabla p_w - \rho_w g\, \boldsymbol{k}, \quad \nabla \cdot \boldsymbol{u}_w = 0. \tag{1.3}$$

Such a system is familiar from classical water-wave theory: the first equation implies $p_a = \text{const.}$, and when the air domain is connected, with an interface described as a graph $z = \eta(x, t)$ over all the x values, this is the well-known free-surface dynamic boundary condition of constant pressure $p_w = p_a$. Augmented by the kinematic boundary condition for this surface, system (1.3) is well defined and a solution can in principle be computed once appropriate initial conditions are assigned. However, suppose now that the water is in contact with the upper plate, so that the air domain becomes disconnected (see figure 1). In this case, while air pressure will still be constant in each component of the domain, as required by the equation $\nabla p_a = 0$, the values of these constants need not be the same for each air-domain component, in general. This would have an effect on the conservation of the total horizontal momentum of the water

$$\Pi_w = \rho_w \int_{-\infty}^{+\infty} \int_0^{\eta} u_w \, \mathrm{d}z \, \mathrm{d}x, \tag{1.4}$$

since for $\rho_a = 0$ (1.1) now reads (recall that air momentum is zero due to $\rho_a = 0$)

$$\dot{\Pi}_w = -hP_\Delta. \tag{1.5}$$

Thus, if the air domain is connected, $P_\Delta = 0$ and the total horizontal water momentum is conserved. Note that connectedness typically happens in genuine three-dimensional settings for localized initial data, which implies that pressure is uniform at infinity. On the other hand, when disconnectedness occurs (which in three dimensions can be obtained by non-localized data such as an infinite water 'ridge' in contact with the upper plate, or simply by suitably localized data in rectangular pipes), by (1.5) the water momentum may not be conserved as a pressure imbalance $P_\Delta \neq 0$ between different air domains can exist.

In the air–water case, this phenomenon is a sort of 'topological transition', as it only depends on the topology of the air free surface with respect to the boundaries: air pressure maintains the same constant value throughout the channel for as long as the air domain is connected; however, passing to the limit of an initial condition that disconnects the air domain (see figure 1), air pressure may evolve in a non-trivial way. Because of air occupying disconnected domains, it may seem at first sight that different constant pressures for each air domain could be freely imposed. In its simplest setting with zero-velocity initial data (the case discussed in detail in § 2) the water pressure satisfies the Laplace equation, which admits a solution for any values of the air pressure at the left- and right-hand wings of the channel. However, this arbitrariness does not exist for any fixed $\rho_a \neq 0$, when hydrostatic equilibrium at infinity is imposed. Passing to the limit $\rho_a \to 0$ while maintaining this constraint provides an extra boundary condition, as we shall show in § 2 in the context of specific examples. This leads to a well-defined, non-vanishing $\dot{\Pi}_w$ corresponding to initial configurations of channel-confined air–water systems where a finite amount of water located in a portion of the channel disconnects an infinite exterior domain occupied by air.

In § 3 we broaden our perspective, from a more theoretical point of view, in two directions. First we consider momentum evolution under general initial conditions (i.e. with generic initial velocities). We show that, for initial conditions in which the air–water interface is not in contact with the plates, a family of constants of motion related to horizontal momentum is associated with the system. On the other hand, water initial data disconnecting the air domain may either select a specific member within this family, or even prevent the whole family from being conserved if portions of the floor are also dry. Next, these results are framed in a Hamiltonian context. Specifically, we consider the Hamiltonian theory of two-dimensional stratified Euler fluids described in Benjamin (1986). We work with continuous stratifications, and show that the Hamiltonian operator described in Benjamin's paper fails to be antisymmetric when the density is not constant on the bounding plates. This is the continuous counterpart of the disconnection phenomenon for general two-layer systems, and in particular for the air–water case of § 2. The lack of antisymmetry offers a theoretical standpoint for a *topological selection* of conservation laws.

Given the translational invariance of the set-up, even under variable-density boundary values, it is natural to ask whether an alternative variational structure exists, which could reveal conservation laws associated with the translational symmetry. We briefly sketch how such a structure could be implemented, though not in full generality but only for the class of motion identified by means of Clebsch variables, using the variational formalism of Zakharov, Musher & Rubenchik (1985).

In closing this introduction, a few remarks are in order: we will not be concerned in this paper with the issue of how connection and disconnection phenomena can be dynamically achieved in the course of the fluid flow evolution. Our focus is on a neighbourhood of the initial time $t = 0$ for special initial conditions, and on the conclusions that can be drawn from these for the general issue of determining conservation laws. Time evolution of general initial data may ultimately be accessible only by numerical simulations. While these necessarily require non-zero air densities, for general two-layer systems our results may still be used to validate numerical approaches in the limit of high density contrast. In turn, the simulations can be used to confirm the relevancy of this limit for interpreting realistic physical set-ups.

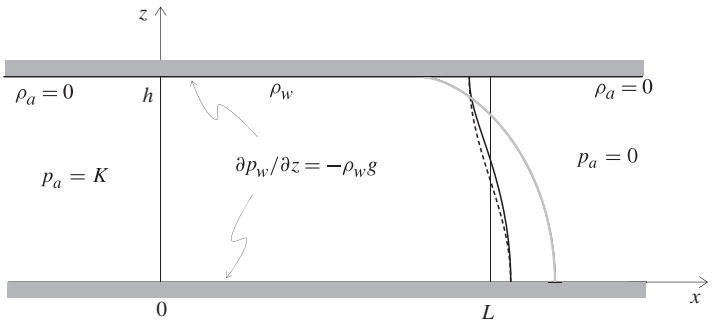

FIGURE 2. The 'boot configuration' for different choices of the right-hand boundary. Solid curves: conformal boundaries x_c^R for exact theory in § 2.1. Dotted line: sinusoidal boundary $x^R(z) \equiv L(1 + \varepsilon \cos(\pi z/h))$ for asymptotics in § 2.2. The figure is produced with actual plots corresponding to the values $h = 1$, $L = 3/2$. Dotted and solid curves: $\varepsilon = \varepsilon_s/\pi \simeq 0.068$. Grey curve: limiting boundary x_c^R for $\varepsilon = \varepsilon_s$. For small ε, $(x_c^R, z_c^R) \sim (x^R(z), z)$, as evidenced by closeness of dotted and solid curves for $\varepsilon = 0.068$.

2. An explicit computation: the 'boot' initial condition

An analytic computation of the initial time evolution of Π_w for a non-connected air domain of generic shape does not seem to be available, in general, even for vanishing initial velocities. To make progress, we study a particular configuration of an air–water system initially at rest at $t = 0$, for which the water domain is sandwiched between non-connected 'dry' infinite channel regions, as sketched in figure 2. We will compute $\dot{\Pi}_w = -hP_\Delta$ for $t = 0$. Since we have assumed zero fluid velocity everywhere at the initial time $t = 0$, taking the divergence of the second (momentum) equation in (1.3) yields, due to the third (incompressibility) equation in (1.3), Laplace's equation for the initial water pressure

$$\nabla^2 p_w = 0. \tag{2.1}$$

As we have seen, the equation for the air pressure $\nabla p_a = 0$ shows that p_a is constant in both domains to the left and the right of the water section, though with possibly different values. Continuity of pressure $p_a = p_w$ at the left- and right-hand interfaces then shows that, on these portions of the water domain, constant Dirichlet boundary conditions are to be enforced. Conversely, the vertical momentum component of the Euler system shows that at the top and bottom plates Neumann boundary conditions for the water pressure are physically required. Thus, we have a well-formulated mixed Dirichlet–Neumann boundary value problem for (2.1) in the water domain Ω_w,

$$p_w(0, z) = K, \qquad p_w(x^R(z), z) = 0, \qquad \left.\frac{\partial p_w}{\partial z}\right|_{z=0,h} = -\rho_w g, \tag{2.2}$$

where we have taken, with no loss of generality, the reference pressure to be zero on the right-hand boundary $x = x^R(z)$, and denoted by K the constant pressure value on the left-hand boundary. A solution p_w of (2.1) with these mixed boundary conditions can always be found for any value of K, leading to an unphysical indeterminacy for this problem (without a mechanism to establish such left-pressure forcing for any finite value of the air density). In particular, $\dot{\Pi}_w = -hP_\Delta \equiv hK$ for any constant K. Thus, a selection mechanism for K is needed to resolve the indeterminacy. This can be found by studying the limit $\rho_a \to 0$ more closely. For a two-fluid system initially at rest,

with $\rho_a \neq 0$, continuity of the pressure and jump conditions of its normal derivative have to be assigned at the interface $\partial\Omega_w$,

$$0 = (p_a - p_w)|_{\partial\Omega_w}, \quad 0 = \left(\frac{1}{\rho_a}\frac{\partial p_a}{\partial n} - \frac{1}{\rho_w}\frac{\partial p_w}{\partial n}\right)\bigg|_{\partial\Omega_w}. \tag{2.3}$$

The second relation follows from the continuity of normal accelerations. When ρ_a vanishes, the jump condition is ill defined and needs to be properly interpreted. This can be done as follows. For non-zero ρ_a and vanishing initial velocities, p_a satisfies the Laplace equation $\nabla^2 p_a = 0$ in each component of the air domain. Thus, the gradient of air pressure ∇p_a is a solenoidal field and its flux across the boundaries is zero:

$$\int_0^h \mathrm{d}z\, \frac{\partial p_a}{\partial x}\bigg|_{x=0} + \int_{-\infty}^0 \mathrm{d}x\, \frac{\partial p_a}{\partial z}\bigg|_{z=h} - \int_{-\infty}^0 \mathrm{d}x\, \frac{\partial p_a}{\partial z}\bigg|_{z=0} - \int_0^h \mathrm{d}z\, \frac{\partial p_a}{\partial x}\bigg|_{x=-\infty} = 0. \tag{2.4}$$

The top and bottom boundary and asymptotic conditions ($\partial_x p_a \to 0$ as $x \to -\infty$) imply

$$\int_0^h \mathrm{d}z\, \frac{\partial p_a}{\partial x}\bigg|_{x=0} = 0. \tag{2.5}$$

From the second condition in (2.3) we find that the same holds for the water pressure. This holds for any value of ρ_a, however small, and hence it is natural to maintain this constraint in the limit $\rho_a \to 0$. Thus, the Laplace equation for the water section must be supplemented, along with (2.2), with the integral consistency condition

$$\int_0^h \mathrm{d}z\, \frac{\partial p_w}{\partial x}\bigg|_{x=0} = 0. \tag{2.6}$$

The constant K will then be selected by enforcing (2.6), thereby determining the value of the pressure in the left-hand air domain solely in terms of the solution to the water problem.

We shall compute this constant value in two cases. The first will be an exact result for a special one-parameter family of conformal maps of rectangles into the domain shapes sketched in figure 2. The second case will be an asymptotic result for general small deviations from a rectangular configuration.

2.1. *An exact solution via conformal mapping*

Consider the conformal mapping (see e.g. Howard & Yu 2007)

$$x = \frac{h}{\pi}\xi + \frac{\varepsilon L}{\sinh(\pi L/h)}\sinh\xi\cos\eta, \quad z = \frac{h}{\pi}\eta + \frac{\varepsilon L}{\sinh(\pi L/h)}\cosh\xi\sin\eta. \tag{2.7}$$

The rectangular domain $0 < \xi < \pi L/h$, $0 < \eta < \pi$ is mapped into a version of the 'boot' of figure 2, with the curved right-hand boundary defined parametrically by

$$x_c^R(\eta) = L + \varepsilon L\cos\eta, \quad z_c^R(\eta) = \frac{h}{\pi}\eta + \varepsilon L\sin\eta\coth(\pi L/h). \tag{2.8}$$

The value of the parameter ε is arbitrary in the range $0 \leqslant \varepsilon \leqslant \varepsilon_s = h\tanh(L\pi/h)/L\pi$. The function $\tilde{p}_w(\xi,\eta) \equiv p_w(x(\xi,\eta), z(\xi,\eta))$, with the conformal map $x(\xi,\eta)$ and $z(\xi,\eta)$ defined by (2.7), satisfies the Laplace equation in the (ξ,η)-domain. The boundary conditions are

$$\tilde{p}_w(0,\eta) = K, \quad \tilde{p}_w(\pi L/h,\eta) = 0, \quad 0 < \eta < \pi, \tag{2.9}$$

and

$$\frac{\partial \tilde{p}_w}{\partial \eta}(\xi, 0) = -g\rho_w \frac{\partial z}{\partial \eta}(\xi, 0) = -g\rho_w \left(\frac{h}{\pi} + \frac{\varepsilon L \cosh \xi}{\sinh(\pi L/h)} \right), \tag{2.10a}$$

$$\frac{\partial \tilde{p}_w}{\partial \eta}(\xi, \pi) = -g\rho_w \frac{\partial z}{\partial \eta}(\xi, \pi) = -g\rho_w \left(\frac{h}{\pi} - \frac{\varepsilon L \cosh \xi}{\sinh(\pi L/h)} \right), \quad 0 < \xi < \pi L/h. \tag{2.10b}$$

The corresponding solution is given by

$$\tilde{p}_w(\xi, \eta) = K \left(1 - \frac{h}{\pi L} \xi \right) + \sum_{n=1}^{\infty} c_n(\eta) \sin(\kappa_n \xi), \quad \kappa_n \equiv nh/L, \tag{2.11}$$

provided the $c_n(\eta)$ satisfy the boundary value problem

$$c_n'' - \kappa_n^2 c_n = 0, \quad c_n'(0) = \varepsilon_n^+, \quad c_n'(\pi) = \varepsilon_n^-, \tag{2.12}$$

where the $\varepsilon_n^{\pm}$ are the Fourier coefficients in the series expression

$$-g\rho_w \left(\frac{h}{\pi} \pm \frac{\varepsilon L \cosh \xi}{\sinh(\pi L/h)} \right) = \sum_{n=1}^{\infty} \varepsilon_n^{\pm} \sin(\kappa_n \xi). \tag{2.13}$$

Hence, these coefficients are given by

$$\varepsilon_n^{\pm} = \frac{2}{\pi} g\rho_w h \left(\frac{(-1)^n - 1}{n\pi} \mp \frac{\varepsilon L h n}{L^2 + h^2 n^2} ((-1)^n \coth(\pi L/h) + \operatorname{cosech}(\pi L/h)) \right), \tag{2.14}$$

and the solution of the boundary value problem (2.12) turns out to be

$$c_n(\eta) = \frac{1}{\kappa_n \sinh(\kappa_n \pi)} \left(\varepsilon_n^- \cosh(\kappa_n \eta) - \varepsilon_n^+ \cosh(\kappa_n(\pi - \eta)) \right). \tag{2.15}$$

In order to find K, we have to impose the constraint (2.6), which takes the form

$$\int_0^{\pi} z_\eta \mathrm{d}\eta \, \frac{1}{x_\xi} \frac{\partial \tilde{p}_w}{\partial \xi} \bigg|_{\xi=0} = 0. \tag{2.16}$$

Since $z_\eta = x_\xi$, this yields

$$\frac{h}{L} K = \sum_{n=1}^{\infty} \kappa_n \int_0^{\pi} \mathrm{d}\eta \, c_n(\eta) = \sum_{n=1}^{\infty} \frac{1}{\kappa_n} (\varepsilon_n^- - \varepsilon_n^+), \tag{2.17}$$

where we have used (2.12). The sum can be computed explicitly, giving the pressure along the left-hand boundary in closed form,

$$K = \frac{2}{\pi} g\rho_w L \varepsilon \tanh \left(\frac{\pi L}{2h} \right). \tag{2.18}$$

The maximal parameter value $\varepsilon = \varepsilon_s$ corresponds to

$$K = \frac{2}{\pi^2} g\rho_w h \tanh \left(\frac{L\pi}{h} \right) \tanh \left(\frac{L\pi}{2h} \right), \tag{2.19}$$

with non-zero limiting value

$$K_\infty = \frac{2}{\pi^2} g\rho_w h \tag{2.20}$$

as $L \to \infty$ (with h fixed). This happens despite the fact that in this limit water fills the entire right-hand wing of the channel, which at first sight could be viewed as a dam-breaking configuration. However, for a genuine dam-breaking set-up the initial layer-mean pressure difference is zero (Camassa *et al.* 2013); this provides an example where a naive interpretation of a geometrical limit can lead to incorrect conclusions, and further shows how such limits must be carefully treated.

2.2. *Generic small perturbations of rectangular domains*

The preceding calculation is exact within the special class of domains from the conformal map (2.7). Next, we outline the computation of the pressure differential K for generic small deviations from the rectangular configuration $(x, z) \in [0, L] \times [0, h]$ of the water domain. We let the right-hand boundary of the water domain be $x^R(z) = L + L\varepsilon\beta(z)$, with the parameter ε now chosen to be small, $0 < \varepsilon \ll 1$, and $\beta(z)$ a smooth function in $[0, h]$. We define $x^+ = x^R(0)$, $x^- = x^R(h)$, and we study the asymptotics for $\varepsilon \to 0$. A general approach to handle such problems goes back to the variational formulation of Hadamard (see e.g. Craig & Sulem 1993); however a direct approach is self-contained and avoids adapting the general framework to our particular set of boundary conditions.

Let us consider the Green function G for the water domain, which satisfies

$$\nabla^2_{(x,z)} G(x, z; \xi, \zeta) = \delta(x - \xi)\delta(z - \zeta), \tag{2.21}$$

with boundary conditions

$$\frac{\partial G}{\partial z}(x, 0; \xi, \zeta) = \frac{\partial G}{\partial z}(x, h; \xi, \zeta) = 0, \quad G(0, z; \xi, \zeta) = G(x^R(z), z; \xi, \zeta) = 0. \tag{2.22}$$

The corresponding third Green identity for this case reads

$$\begin{aligned} p_w(\xi, \zeta) \;=\; & \rho_w g \left(\int_0^{x^-} \mathrm{d}x \; G(x, h; \xi, \zeta) - \int_0^{x^+} \mathrm{d}x \; G(x, 0; \xi, \zeta) \right) \\ & - K \int_0^h \mathrm{d}z \; \frac{\partial G}{\partial x}(0, z; \xi, \zeta). \end{aligned} \tag{2.23}$$

The consistency condition (2.6) then leads to

$$\begin{aligned} 0 \;=\; & -K \int_0^h \mathrm{d}\zeta \int_0^h \mathrm{d}z \, \frac{\partial^2 G}{\partial \xi \, \partial x}(0, z; 0, \zeta) \\ & + \rho_w g \int_0^h \mathrm{d}\zeta \left(\int_0^{x^-} \mathrm{d}x \, \frac{\partial G}{\partial \xi}(x, h; 0, \zeta) - \int_0^{x^+} \mathrm{d}x \, \frac{\partial G}{\partial \xi}(x, 0; 0, \zeta) \right). \end{aligned} \tag{2.24}$$

This formula gives the value K of the pressure in the left-hand air domain in terms of G. Expanding the Green function as $G = G_0 + \varepsilon G_1 + o(\varepsilon)$ yields

$$\nabla^2_{(x,z)} G_0(x, z; \xi, \zeta) = \delta(x - \xi)\delta(z - \zeta), \quad \nabla^2_{(x,z)} G_1(x, z; \xi, \zeta) = 0. \tag{2.25}$$

Boundary conditions for G_0 and G_1 follow from (2.22) and

$$G(x^R(z), z; \xi, \zeta) = G_0(L, z; \xi, \zeta) + \varepsilon \left[G_1(L, z; \xi, \zeta) + L\beta(z) \frac{\partial G_0}{\partial x}(L, z; \xi, \zeta) \right] + o(\varepsilon), \tag{2.26}$$

establishing a recursion between solutions at each order in powers of ε. In particular,

$$G_0(L, z; \xi, \zeta) = 0, \quad G_1(L, z; \xi, \zeta) = -L\beta(z)\frac{\partial G_0}{\partial x}(L, z; \xi, \zeta). \tag{2.27}$$

Hence G_0 is the Green function in the rectangle $[0, L] \times [0, h]$ with boundary conditions

$$\frac{\partial G_0}{\partial z}(x, 0; \xi, \zeta) = \frac{\partial G_0}{\partial z}(x, h; \xi, \zeta) = 0, \quad G_0(0, z; \xi, \zeta) = G_0(L, z; \xi, \zeta) = 0, \tag{2.28}$$

which can be expressed as $G_0(x, y; \xi, \zeta) = \sum_{n=0}^{\infty} g_n^{(0)}(x; \xi)\cos(k_n z)\cos(k_n \zeta)$, where

$$g_0^{(0)}(x; \xi) = \tfrac{1}{2h}\left(|x - \xi| + \tfrac{2}{L}x\xi - (x + \xi)\right) \tag{2.29a}$$

and for $n \geqslant 1$, $k_n \equiv n\pi/h$,

$$g_n^{(0)}(x; \xi) = -\frac{\mathrm{e}^{-k_n|x-\xi|}}{n\pi} + \frac{\cosh(k_n(x + \xi - L)) - \mathrm{e}^{-k_n L}\cosh(k_n(x - \xi))}{n\pi \sinh(k_n L)}. \tag{2.29b}$$

From (2.25) and (2.27), the first-order correction term G_1 to the Green function must be a harmonic function satisfying the mixed boundary conditions

$$\frac{\partial G_1}{\partial z}(x, 0; \xi, \zeta) = \frac{\partial G_1}{\partial z}(x, h; \xi, \zeta) = 0, \tag{2.30a}$$

$$G_1(0, z; \xi, \zeta) = 0, \quad G_1(L, z; \xi, \zeta) = -L\beta(z)\tfrac{\partial G_0}{\partial x}(L, z; \xi, \zeta). \tag{2.30b}$$

For a solution of the form $G_1(x, z; \xi, \zeta) = \sum_{n=0}^{\infty} g_n^{(1)}(x; \xi, \zeta)\cos(k_n z)$, the Dirichlet boundary conditions (2.30*b*) for G_1 yield

$$g_0^{(1)}(x; \xi, \zeta) = f_0(\xi, \zeta)\, x/L, \quad g_n^{(1)}(x; \xi, \zeta) = \frac{\sinh(k_n x)}{\sinh(k_n L)} f_n(\xi, \zeta), \quad n \geqslant 1, \tag{2.31}$$

in terms of the coefficients f_n of the expansion $G_1(L, z; \xi, \zeta) \equiv \sum_{n=0}^{\infty} f_n(\xi, \zeta)\cos(k_n z)$, whose explicit form can be found from $\beta(z)$ and G_0 through (2.30*b*). If we put $K = K_0 + \varepsilon K_1 + o(\varepsilon)$ in (2.24), then at leading-order we obtain

$$\begin{aligned} K_0 \int_0^h \mathrm{d}\zeta \int_0^h \mathrm{d}z \frac{\partial^2 G_0}{\partial \xi\, \partial x}(0, z; 0, \zeta) \\ = \rho_w g \int_0^h \mathrm{d}\zeta \int_0^L \mathrm{d}x \left(\frac{\partial G_0}{\partial \xi}(x, h; 0, \zeta) - \frac{\partial G_0}{\partial \xi}(x, 0; 0, \zeta)\right). \end{aligned} \tag{2.32}$$

By using (2.29) the integral on the right-hand side vanishes, while that on the left-hand side equals h/L, whence $K_0 = 0$, as expected by symmetry considerations. At the next order in ε (2.24) gives

$$\begin{aligned} K_1 \;=\; & \frac{\rho_w g L}{h} \int_0^h \mathrm{d}\zeta \int_0^L \mathrm{d}x \left(\frac{\partial G_1}{\partial \xi}(x, h; 0, \zeta) - \frac{\partial G_1}{\partial \xi}(x, 0; 0, \zeta)\right) \\ & + \frac{\rho_w g L^2}{h} \int_0^h \mathrm{d}\zeta \left(\beta(h)\frac{\partial G_0}{\partial \xi}(L, h; 0, \zeta) - \beta(0)\frac{\partial G_0}{\partial \xi}(L, 0; 0, \zeta)\right), \end{aligned} \tag{2.33}$$

where the last integral vanishes due to (2.29). Thus K_1 can be computed from the boundary values of G_1. These, in turn, are determined by the profile perturbation $\beta(z)$

(*a*) $\varepsilon = 1/10$ fixed, decreasing ρ_a

	Numerics			Theory
ρ_a	1/10	1/40	1/160	0
P_Δ (conformal boundary)	-4.29×10^{-2}	-5.41×10^{-2}	-5.73×10^{-2}	-5.84×10^{-2}
P_Δ (sinusoidal boundary)	-4.21×10^{-2}	-5.27×10^{-2}	-5.58×10^{-2}	-5.84×10^{-2}

(*b*) $\rho_a = 1/160$ fixed, decreasing ε

	ε	1/10	1/20	1/40
Numerics	P_Δ (conformal boundary)	-5.73×10^{-2}	-2.87×10^{-2}	-1.39×10^{-2}
	P_Δ (sinusoidal boundary)	-5.58×10^{-2}	-2.85×10^{-2}	-1.43×10^{-2}
Theory	P_Δ	-5.84×10^{-2}	-2.92×10^{-2}	-1.46×10^{-2}

(*c*) Maximal conformal map domain $\varepsilon = \varepsilon_s$, decreasing ρ_a

	Numerics			Theory
ρ_a	1/10	1/20	1/40	0
P_Δ (conformal boundary)	−0.116	−0.143	−0.161	−0.185

TABLE 1. Numerical and analytical P_Δ-values at $t = 0$ with water domains specified by the conformal map (2.7) and the sinusoidal boundary $\beta(z) = \cos(\pi z/h)$ (figure 2). Parameters are $L = h = 1$, $\rho_w = 1$, $g = 1$. The aspect ratio of the computational domain is 1:16 with impermeable boundaries at $x = -8, 8$ and $z = 0, 1$. A square grid with 256 points along the vertical is used throughout. The domain left-hand boundary is at $x = 0$. Top table: $\varepsilon = 1/10$ fixed, decreasing ρ_a; middle table: $\rho_a = 1/160$ fixed, decreasing ε; bottom table: maximal conformal map domain $\varepsilon = \varepsilon_s$, decreasing ρ_a.

according to (2.30). For $\beta(z) = \cos(\pi z/h)$ we obtain

$$K = \frac{2}{\pi}\rho_w g \varepsilon L \tanh\left(\frac{\pi L}{2h}\right) + o(\varepsilon), \tag{2.34}$$

which agrees with the exact result (2.18) for the special profiles defined by (2.7). This is in agreement with the fact that boundary profile from the conformal map limits for small ε to this sinusoidal choice of $\beta(z)$ in the definition of $x^R(z)$. In the Appendix, we provide an explicit expression for the case of a step, which can in principle be implemented experimentally by use of removable gates.

2.3. *Numerical validation*

It is interesting to see how general algorithms for computing the time evolution of stratified Euler fluids fare with respect to the above results. These can severely test the limitations of numerical techniques as they require handling simultaneously the limits of infinite channel horizontal lengths and zero densities of one of the fluids. In turn, numerical simulations can help assess the robustness of the asymptotics $\rho_a \to 0$ for small but finite air density ρ_a. As seen from table 1, computations using the VARDEN algorithm (Almgren *et al.* 1998), following the set-up reported in Camassa *et al.* (2012, 2013), are in reasonable agreement with our analysis, despite finite channel lengths and density ratios.

2.4. *The case of unbounded water domain*

We discuss now how to compute the initial value of the pressure difference P_Δ in the case of figure 3, where the water domain is unbounded and splits the air domain in

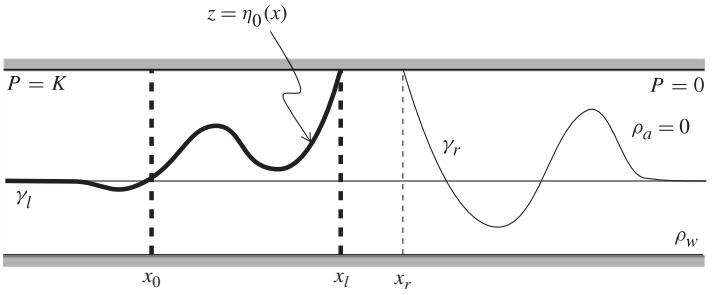

FIGURE 3. Air–water system, with unbounded water domain, uniform hydrostatic equilibrium at infinity, and initial zero velocities. In the limiting case $\rho_a = 0$, condition (2.38) is assumed to hold.

two parts. The velocity field is always supposed to vanish at $t = 0$. When $\rho_a = 0$, we can still put $P_l = K$ and $P_r = 0$, so that the (initial value of the) water pressure p_w turns out to be the unique bounded harmonic function on the water domain satisfying the Dirichlet–Neumann boundary conditions

$$p_w = K \quad \text{at } \gamma_l, \qquad p_w = 0 \quad \text{at } \gamma_r, \qquad \left.\frac{\partial p_w}{\partial z}\right|_{z=0,h} = -\rho_w g, \tag{2.35}$$

where γ_l (resp. γ_r) is the left (resp. right) part of the air–water interface. As in the boot configuration, we will find a selection mechanism to fix the value of K by considering the case $\rho_a \neq 0$ and pointing out a condition on p_w that survives the limit $\rho_a \to 0$. For non-zero ρ_a and vanishing initial velocities, we let $\Omega_w^{x_0}$ (resp. $\Omega_a^{x_0}$) be the subset of the water (resp. air) domain with $x_0 \leqslant x \leqslant x_l$. We also let γ^{x_0} be the subset of the interface with $x_0 \leqslant x \leqslant x_l$. The initial pressures p_w and p_a satisfy the Laplace equation in their domains. Then we can use, as in (2.4), the fact that the flux of the gradient of p_w (resp. p_a) across the boundary of $\Omega_w^{x_0}$ (resp. $\Omega_a^{x_0}$) is zero, to obtain, for $x_0 \leqslant x_l$,

$$-\int_0^{\eta_0(x_0)} \mathrm{d}z \left.\frac{\partial p_w}{\partial x}\right|_{x=x_0} + \int_{\gamma^{x_0}} \mathrm{d}s \frac{\partial p_w}{\partial n} + \int_0^h \mathrm{d}z \left.\frac{\partial p_w}{\partial x}\right|_{x=x_l} - \int_{x_0}^{x_l} \mathrm{d}x \left.\frac{\partial p_w}{\partial z}\right|_{z=0} = 0, \tag{2.36a}$$

$$-\int_{\eta_0(x_0)}^h \mathrm{d}z \left.\frac{\partial p_a}{\partial x}\right|_{x=x_0} - \int_{\gamma^{x_0}} \mathrm{d}s \frac{\partial p_a}{\partial n} + \int_{x_0}^{x_l} \mathrm{d}x \left.\frac{\partial p_a}{\partial z}\right|_{z=h} = 0, \tag{2.36b}$$

where $\partial/\partial n$ is the normal derivative in the direction from water to air, and we have denoted with $z = \eta_0(x)$ the function describing the interface at $t = 0$. After dividing the first (resp. second) equation by ρ_w (resp. ρ_a), summing, and using the boundary conditions (at $z = 0$, h) and the jump conditions (2.3) of the normal derivatives, we obtain that

$$\frac{1}{\rho_w}\int_0^{\eta_0(x_0)} \mathrm{d}z \left.\frac{\partial p_w}{\partial x}\right|_{x=x_0} + \frac{1}{\rho_a}\int_{\eta_0(x_0)}^h \mathrm{d}z \left.\frac{\partial p_a}{\partial x}\right|_{x=x_0} = \frac{1}{\rho_w}\int_0^h \mathrm{d}z \left.\frac{\partial p_w}{\partial x}\right|_{x=x_l} \tag{2.37}$$

for all $x_0 \leqslant x_l$. Since $\partial_x p_a$ and $\partial_x p_w$ go to zero as $x \to -\infty$, we obtain

$$\int_0^h \mathrm{d}z \left.\frac{\partial p_w}{\partial x}\right|_{x=x_l} = 0. \tag{2.38}$$

(It is very easy to show that this is also true with x_l replaced by any $x \in [x_l, x_r]$.) It coincides with the consistency condition (2.6) of the boot case, and the conclusion is now the same. Namely, condition (2.38) holds for any non-zero value of ρ_a, so we impose this constraint in the limit $\rho_a \to 0$. Hence, we add it to the boundary conditions (2.35) for the Laplace equation in the water domain to select the constant K. The value of the (initial) pressure in the left-hand air domain is therefore determined by the solution to the water problem.

3. Topological selection

As we have seen from (1.5), when the air domain is connected, the total horizontal momentum of the air–fluid system

$$\Pi = \Pi_w = \rho_w \int_{-\infty}^{+\infty} \mathrm{d}x \int_0^{\eta(x,t)} \mathrm{d}z\ u(x, z) \tag{3.1}$$

is conserved, since $P_\Delta = 0$ in this case. In order to deal with the disconnected air-domain case, it is useful to define the boundary fields

$$\lim_{z\to 0^+} u(x, z, t) \equiv u^-(x, t), \qquad \lim_{z\to h^-} u(x, z, t) \equiv u^+(x, t), \tag{3.2}$$

and similarly for all other dependent variables in the Euler system. With the definition of boundary variables (3.2) and their analogue for ρ and p, it is easy to see that the corresponding 'lower-boundary momentum' Π^- from the definition

$$\Pi^\pm = h \int_{-\infty}^{+\infty} \mathrm{d}x\, \rho^\pm u^\pm(x, t) \tag{3.3}$$

is a time-invariant quantity. In fact, the boundary condition $w^-(x, t) = 0$ implies

$$\dot{\Pi}^- = -h \int_{-\infty}^{+\infty} \mathrm{d}x\, (\rho_w u^- u^-_x + p^-_x) = -h(p^-(+\infty) - p^-(-\infty)) = -hP_\Delta, \tag{3.4}$$

due to the assumed hydrostatic boundary conditions as $|x| \to \infty$. Thus, if the air domain is connected, so that $P_\Delta = 0$, Π^- is conserved as well. This allows us to define a one-parameter family of conserved quantities,

$$\Pi_\alpha \equiv \Pi + \alpha \Pi^-. \tag{3.5}$$

Remarkably, while for a disconnected air domain when $P_\Delta \neq 0$ neither Π nor Π^- are separately conserved (cf. (1.5) and (3.4)), the member of the family with $\alpha = -1$ is,

$$\dot{\Pi}_{-1} = \dot{\Pi} - \dot{\Pi}^- = 0. \tag{3.6}$$

Hence, the topological change of the air domain from connected to disconnected results in the collapse of a whole family of conserved quantities (3.5) into the single quantity (3.6). We may call this phenomenon 'topological selection' of horizontal momentum.

The upper-boundary counterpart of Π^- is worth considering as well. While for air–water systems with connected air-domains Π^+ is clearly zero, this is no longer the case for disconnected domains. The water dynamics may generate a non-vanishing upper-boundary momentum contribution in regions where water is in contact with the upper lid. For instance, when the contact region corresponds to the interval (see figure 1) $z = h$, $x_l < x < x_r$, the integral in the definition of the upper-boundary

momentum Π^+ is taken over the interval and evolves as

$$\begin{aligned}\dot{\Pi}^+ &= h\rho_w\left(\dot{x}_r u^+(x_r,t) - \dot{x}_l u^+(x_l,t) - \int_{x_l}^{x_r} \mathrm{d}x\,(u^+ u_x^+ + p_x^+/\rho_w)\right)\\ &= -hP_\Delta + \frac{h\rho_w}{2}\left((u^+(x_r(t),t))^2 - (u^+(x_l(t),t))^2\right), \end{aligned} \tag{3.7}$$

since $\dot{x}_r = u^+(x_r,\ t)$ (resp. $\dot{x}_l = u^+(x_l,\ t)$), and $p^+(x_r,\ t) - p^+(x_l,\ t) = P_\Delta(t)$. The counterpart of (3.6) is then

$$\dot{\Pi} - \dot{\Pi}^+ = -\frac{h\rho_w}{2}((u^+(x_r(t),t))^2 - (u^+(x_l(t),t))^2), \tag{3.8}$$

which is not a conservation law in general. A notable exception is offered by the case of left–right symmetric initial interface and zero initial velocities, since time evolution preserves the left–right symmetry and $|u^+(x_r(t),t)| = |u^+(x_l(t),t)|$ at all times.

Two further remarks are in order. First, a configuration with a disconnected water domain in the presence of a connected air domain preserves the total momentum Π, while Π^- is not generally conserved. Second, and more importantly, if both water and air domains are disconnected no member of the family (3.5) is conserved, in general.

3.1. *Topological selection for continuous stratifications*

The selection mechanism exemplified by (3.6) admits a natural extension within the Hamiltonian formalisms for a continuously stratified incompressible two-dimensional Euler fluid (see e.g. Zakharov *et al.* 1985; Benjamin 1986; Morrison 1998).

Let us briefly describe Benjamin's formalism. The incompressible Euler equations are written in terms of physical quantities, the density field $\rho(x,z,t)$ and the density-weighted vorticity $\sigma(x,z,t) = (\rho w)_x - (\rho u)_z$, as

$$\rho_t + \rho_x\psi_z - \rho_z\psi_x = 0, \tag{3.9a}$$

$$\sigma_t + \sigma_x\psi_z - \sigma_z\psi_x + \rho_x(g - \boldsymbol{u}\cdot\boldsymbol{u}_z) + \rho_z\boldsymbol{u}\cdot\boldsymbol{u}_x = 0. \tag{3.9b}$$

Here the stream function $\psi(\rho,\sigma)$, and the ensuing velocity field $u = \psi_z$ and $w = -\psi_x$, should be interpreted as a shorthand notation for the solution of the elliptic problem

$$\nabla\cdot(\rho\nabla\psi) = -\sigma. \tag{3.10}$$

As pointed out by Benjamin, an appropriate boundary condition for ψ is that of homogeneous Dirichlet data, $\psi = 0$. This ensures that a unique solution ψ of (3.10) can be found for any assigned density field ρ. The functions ρ and σ are the fundamental variables for a Hamiltonian structure of the incompressible Euler equations. The Hamiltonian H for system (3.9) is

$$H = \int_{-\infty}^{+\infty}\int_{z_-}^{z_+}\left(\frac{\rho}{2}|\nabla\psi|^2 + gz(\rho-\rho_0)\right)\mathrm{d}z\,\mathrm{d}x, \tag{3.11}$$

where $\rho_0 = \rho_0(z)$ is the density of a stable hydrostatic equilibrium reference configuration for the fluid as $|x|\to\infty$. Henceforth we consider for convenience a general vertical coordinate origin with the bottom and top plates located at $z = z_-, z_+$ with total height of the channel $h = z_+ - z_-$.

Equations of motion (3.9) can then be obtained by means of non-canonical Poisson brackets, defined for general functionals $F[\rho, \sigma]$, $G[\rho, \sigma]$ by

$$\{F, G\} \equiv -\int_{-\infty}^{+\infty}\int_{z_-}^{z_+} (\delta_\rho F, \delta_\sigma F) \begin{pmatrix} 0 & \rho_x\partial_z - \rho_z\partial_x \\ \rho_x\partial_z - \rho_z\partial_x & \sigma_x\partial_z - \sigma_z\partial_x \end{pmatrix} \begin{pmatrix} \delta_\rho G \\ \delta_\sigma G \end{pmatrix} \mathrm{d}z\ \mathrm{d}x. \tag{3.12}$$

In fact, the variational differential of the Hamiltonian (3.11) is

$$\left(\delta_\rho H, \delta_\sigma H\right) = \left(g\,z - |\nabla\psi|^2/2,\, \psi\right). \tag{3.13}$$

Note that boundary terms generated by the variation are automatically eliminated by the condition $\psi = 0$, as

$$\begin{aligned} &H[\rho + \delta\rho, \sigma + \delta\sigma] - H[\rho, \sigma] \\ &\quad = \int_{-\infty}^{+\infty}\int_{z_-}^{z_+} \left(\left(g\,z - |\nabla\psi|^2/2\right)\delta\rho + \psi\ \delta\sigma + \nabla\cdot(\psi\ \delta(\rho\nabla\psi))\right) \mathrm{d}z\,\mathrm{d}x. \end{aligned} \tag{3.14}$$

The generator of horizontal translations is easily recognized to be the functional

$$\mathscr{I}_B = \int_{-\infty}^{+\infty}\int_{z_-}^{z_+} z\sigma\,(x, z)\,\mathrm{d}z\,\mathrm{d}x. \tag{3.15}$$

This is a member of the family of constants of motion identified (along with the associated symmetries) in Benjamin (1986).

The Poisson bracket (3.12) admits a wide class of Casimir functionals (namely, functionals $C[\rho, \sigma]$ such that $\{\cdot, C\} = 0$). They are given by

$$\mathscr{C}^{\alpha,\beta} = \int_{-\infty}^{+\infty}\int_{z_-}^{z_+} (\alpha(\rho)\sigma + \beta(\rho))\mathrm{d}z\,\mathrm{d}x \tag{3.16}$$

for every pair of functions $\alpha(\rho)$ and $\beta(\rho)$. Obviously, as in any Hamiltonian setting, Casimir functionals define constants of the motion (though unlike standard conserved quantities, they are associated with trivial symmetries).

As it stands the Hamiltonian formalism ensuing from (3.12) falls apart with configurations for which ρ (and/or σ) is non-constant along the top and bottom plates (as in the idealized air–water configurations of § 2, which, in their continuously stratified extension, imply that some of the isopycnals intersect the bounding plates). In particular, the bracket defined by (3.12) fails to be antisymmetric in general due to boundary contributions in (3.12) dependent on $\rho_x^{\pm}$ and $\sigma_x^{\pm}$.

A straightforward computation shows that the lack of antisymmetry of the Poisson bracket is

$$S(F, G) \equiv \{F, G\} + \{G, F\} = -\int_{-\infty}^{+\infty} (\delta_\rho F, \delta_\sigma F) \begin{pmatrix} 0 & \rho_x \\ \rho_x & \sigma_x \end{pmatrix} \begin{pmatrix} \delta_\rho G \\ \delta_\sigma G \end{pmatrix} \Big|_{z_-}^{z_+} \mathrm{d}x, \tag{3.17}$$

where, hereafter,

$$\mathscr{A}\,|_{z_-}^{z_+} \equiv \mathscr{A}(x, z_+) - \mathscr{A}(x, z_-). \tag{3.18}$$

Despite this antisymmetry defect, equations of motion (3.9) can still be written as those from the Hamiltonian structure (3.11)–(3.12),

$$\left.\begin{aligned}\rho_t &= \{\rho, H\} = \rho_z \left(\frac{\delta H}{\delta \sigma}\right)_x - \rho_x \left(\frac{\delta H}{\delta \sigma}\right)_z,\\ \sigma_t &= \{\sigma, H\} = \rho_z \left(\frac{\delta H}{\delta \rho}\right)_x - \rho_x \left(\frac{\delta H}{\delta \rho}\right)_z + \sigma_z \left(\frac{\delta H}{\delta \sigma}\right)_x - \sigma_x \left(\frac{\delta H}{\delta \sigma}\right)_z.\end{aligned}\right\} \tag{3.19}$$

We stress that this form of the motion equations, which is the one provided by Benjamin (1986) for constant boundary values of ρ (and, in general, σ), continues to hold for non-constant boundary field configurations because of the choice of homogeneous Dirichlet data for the stream function ψ (i.e. vanishing at $z = z_{\pm}$), since under this condition the variational differential of H is still given by (3.13). The main consequence of the breakdown of the Hamiltonian formalism due to the lack of bracket antisymmetry is the loss of the correspondence between symmetries and constants of the motion. In general, a quantity which is conserved by motion with constant boundary fields may very well change in time in the case of variable boundary fields.

An example is the family of Casimirs $\mathscr{C}^{\alpha,\beta}$. We have

$$\dot{\mathscr{C}}^{\alpha,\beta} = \int_{-\infty}^{+\infty} \int_{z_-}^{z_+} \left(\delta_\rho \mathscr{C}^{\alpha,\beta} \rho_t + \delta_\sigma \mathscr{C}^{\alpha,\beta} \sigma_t\right) \mathrm{d}z\, \mathrm{d}x = \{\mathscr{C}^{\alpha,\beta}, H\}, \tag{3.20}$$

where the last equality is due to (3.19). By definition (3.17) we have

$$\{\mathscr{C}^{\alpha,\beta}, H\} = -\{H, \mathscr{C}^{\alpha,\beta}\} + S(\mathscr{C}^{\alpha,\beta}, H). \tag{3.21}$$

The first term on the right-hand side vanishes since the variational differential of $\mathscr{C}^{\alpha,\beta}$ annihilates point-wise the integral kernel operator in the definition of the bracket (3.12). Thanks to the homogeneous boundary conditions for the stream function, the antisymmetry defect $S(\mathscr{C}^{\alpha,\beta}, H)$ reduces in this case to

$$S(\mathscr{C}^{\alpha,\beta}, H) = -\int_{-\infty}^{+\infty} \rho_x \delta_\sigma \mathscr{C}^{\alpha,\beta} \delta_\rho H \Big|_{z_-}^{z_+} \mathrm{d}x = \frac{1}{2} \int_{-\infty}^{+\infty} \rho_x \alpha |\nabla \psi|^2 \Big|_{z_-}^{z_+} \mathrm{d}x. \tag{3.22}$$

In terms of physical variables this is

$$\dot{\mathscr{C}}^{\alpha,\beta} = \frac{1}{2} \int_{-\infty}^{+\infty} \alpha \rho_x u^2 \Big|_{z_-}^{z_+} \mathrm{d}x. \tag{3.23}$$

Similarly, the generator of horizontal translations (3.15) may fail to be conserved when the field densities vary along the plates. Indeed, arguing as above (or directly by using the equations of motion), it is easy to show that

$$\dot{\mathscr{I}}_B = z_+ J^+ - z_- J^-, \tag{3.24}$$

where we have defined for simplicity the boundary quantities $J^{\pm}$ as

$$J^{\pm} \equiv \frac{1}{2} \int_{-\infty}^{+\infty} \rho_x^{\pm} (u^{\pm})^2 \, \mathrm{d}x. \tag{3.25}$$

We remark that the time derivative of one of the simplest Casimir of the family, namely

$$\mathscr{C} \equiv \mathscr{C}^{(1,0)} = \int_{-\infty}^{+\infty} \int_{z_-}^{z_+} \sigma \, \mathrm{d}z \, \mathrm{d}x, \tag{3.26}$$

can be written by means of the quantities $J^{\pm}$ as

$$\dot{\mathscr{C}} = J^+ - J^-. \tag{3.27}$$

Thus, as $J^{\pm}$ are generally non-zero if ρ varies along the plates, $\mathscr{I}_B$ and $\mathscr{C}$ are no longer conserved for generic configurations. Of course, non-constant ρ implies that ρ-level sets intersect the boundaries, which effectively separates the fluid domain into different topological regions. (Note that disconnected configurations cannot be obtained by continuous deformation of a rest state in hydrostatic equilibrium.) Just as in the particular air–water case, the analogue of the topological selection mechanism may occur if the density is constant along one of the plates (but not both). For instance, if ρ is constant along the lower plate, then $\rho_x^- = 0$ and J^- is zero. From (3.24) and (3.27) it follows that $\mathscr{I}_B - z_+\mathscr{C}$ is conserved. Thus, we have a complete analogy with the results for the air–water sharp stratification described in the first part of this section.

3.2. *Clebsch formulation*

Even with non-constant ρ along the plates, the channel set-up is invariant under horizontal translations, and one could ask whether a related conservation law can nonetheless be found. We discuss this issue for a class of fluid motions that admits a special variational representation (cf. Zakharov & Kuznetsov 1997). This set-up relies on so-called Clebsch variables for two-dimensional Euler equations and, in particular, allows for non-zero vorticity only in those regions where the density is not constant (for a comparison with Benjamin's formalism, see Camassa *et al.* 2013). Thus, an additional pair of dependent variables (λ, ϕ) is introduced as Lagrange multipliers in the Lagrangian obtained by the difference of kinetic and potential energy of the system,

$$L = \int_{-\infty}^{+\infty} \int_{z_-}^{z_+} \left(\tfrac{1}{2}\rho|\boldsymbol{u}|^2 - \rho g z + \phi \boldsymbol{\nabla}\cdot\boldsymbol{u} + \lambda(\rho_t + \boldsymbol{\nabla}\cdot(\rho\,\boldsymbol{u})) \right) \mathrm{d}z \, \mathrm{d}x. \tag{3.28}$$

(Note that we have slightly altered the form of the Lagrangian with respect to the one in Zakharov & Kuznetsov (1997), by using the full version of the mass conservation equation $\rho_t + \boldsymbol{\nabla}\cdot(\rho\boldsymbol{u}) = 0$, rather than its incompressible version $\rho_t + \boldsymbol{u}\cdot\boldsymbol{\nabla}\rho = 0$.)

Variation of the action corresponding to Lagrangian (3.28) yields evolution equations

$$\left.\begin{array}{ll} \rho_t + \boldsymbol{\nabla}\cdot(\rho\,\boldsymbol{u}) = 0, & \lambda_t + \boldsymbol{u}\cdot\boldsymbol{\nabla}\lambda - \tfrac{1}{2}|\boldsymbol{u}|^2 + g\,z = 0, \\ \boldsymbol{\nabla}\cdot\boldsymbol{u} = 0, & \rho\boldsymbol{u} - \boldsymbol{\nabla}\phi - \rho\boldsymbol{\nabla}\lambda = 0. \end{array}\right\} \tag{3.29}$$

These equations need to be augmented by the appropriate boundary conditions. These can be retrieved from the variational formulation as follows: variations for the velocity $\boldsymbol{u} + \delta\boldsymbol{u}$ must satisfy the same boundary conditions as $\boldsymbol{u}$. Hence, in order to be admissible for the class of fluid motions under consideration, variations $\delta\boldsymbol{u}$ are subject to the homogeneous version of the $\boldsymbol{u}$-conditions at the boundaries of the fluid domain. In contrast, variations $\rho + \delta\rho$ are not assigned special values at the top and bottom plates, though $\partial_x(\delta\rho) \to 0$ as $|x| \to \infty$ in order to leave the far-end density field in hydrostatic equilibrium. The boundary terms from the variation of the action

generated by (3.28) are

$$(\phi + \lambda\rho)\, \boldsymbol{n} \cdot \delta\boldsymbol{u} + (\lambda\, \boldsymbol{n} \cdot \boldsymbol{u})\, \delta\rho, \tag{3.30}$$

and the first term vanishes because $\boldsymbol{n} \cdot \delta\boldsymbol{u} = 0$, with $\boldsymbol{n}$ the normal to the boundary of the fluid domain. When this is a channel, the boundary conditions generated by ρ-variations are therefore either

$$w = 0 \quad \text{at } z = z_{\pm} \quad \text{and} \quad u = 0 \quad \text{as } x \to \pm\infty, \tag{3.31}$$

or

$$\lambda = 0 \quad \text{at } z = z_{\pm} \quad \text{and as} \quad x \to \pm\infty. \tag{3.32}$$

Of these, only (3.31) correspond to the physical boundary conditions for Euler flows in a channel. As to the structure of the resulting evolution equations, it must be stressed that solutions of system (3.29) are also solutions of the original Euler equations (1.2) in two dimensions, but the converse is not necessarily true; for instance the homogeneous fluid ρ =const. case yields irrotational solutions $\rho\,\boldsymbol{u} = \boldsymbol{\nabla}(\phi + \rho\lambda)$ only. Specifically, taking the gradient of the second equation in system (3.29), and the convective derivative $\partial/\partial t + \boldsymbol{u} \cdot \boldsymbol{\nabla} \equiv \mathrm{D}/\mathrm{D}t$ of the last equation, yields

$$\frac{\mathrm{D}(\rho\boldsymbol{u})}{\mathrm{D}t} = \boldsymbol{\nabla}\left(\frac{\mathrm{D}\phi}{\mathrm{D}t}\right) - \rho g\, \boldsymbol{k}, \tag{3.33}$$

whence Euler equations follow from identifying

$$\boldsymbol{\nabla}\left(\frac{\mathrm{D}\phi}{\mathrm{D}t}\right) = -\boldsymbol{\nabla} p, \tag{3.34}$$

i.e. the relation between the Euler pressure p and the Clebsch variable ϕ.

We remark that the definition (3.29) of Clebsch variables possesses an inherent indeterminacy consistent with the fact that the fields ϕ and λ are not physically observable quantities *per se*: the two pairs $(\phi,\ \lambda)$, $(\phi',\ \lambda')$ reproduce the same physical observables $\rho\boldsymbol{u}$ and p if they satisfy

$$\boldsymbol{\nabla}(\phi' - \phi) = -\rho\, \boldsymbol{\nabla}(\lambda' - \lambda), \quad \boldsymbol{\nabla}\left(\frac{\mathrm{D}(\phi' - \phi)}{\mathrm{D}t}\right) = 0. \tag{3.35}$$

These can constrain the admissible values of $\phi' - \phi$.

In contrast to the Hamiltonian formulation (3.19), it can be easily shown that the Clebsch variables define a canonical Hamiltonian formulation in which ρ and λ are conjugate variables, evolving according to the system

$$\rho_t = \frac{\delta H}{\delta\lambda}, \quad \lambda_t = -\frac{\delta H}{\delta\rho}, \quad H = \int_{-\infty}^{+\infty}\int_{z_-}^{z_+} \left(\tfrac{1}{2}\rho|\boldsymbol{u}|^2 + g(\rho - \rho_0)\, z\right)\, \mathrm{d}z\, \mathrm{d}x. \tag{3.36}$$

Here $\boldsymbol{u}$ is interpreted as shorthand notation for its definition in (3.29), while ϕ stands for the function of (λ, ρ) defined through the elliptic problem

$$\boldsymbol{\nabla} \cdot \left(\frac{1}{\rho}\boldsymbol{\nabla}\phi\right) = -\nabla^2\lambda, \tag{3.37}$$

which is equivalent to $\boldsymbol{\nabla} \cdot \boldsymbol{u} = 0$. With Neumann boundary conditions and up to constants, ϕ is therefore uniquely defined by inverting an elliptic operator similar to that in (3.10) (for density ρ bounded away from zero everywhere). In terms of these

Clebsch variables, the generator of horizontal translations is

$$\mathscr{I}_{ZK} \equiv \int_{-\infty}^{+\infty} \int_{z_-}^{z_+} \lambda\, \rho_x \,\mathrm{d}z\,\mathrm{d}x. \tag{3.38}$$

According to Noether's theorem, it is a conserved quantity. Up to an overall constant depending only on the initial values of boundary fields, $\mathscr{I}_{ZK}$ equals $\mathscr{I}_B$ for constant ρ along the boundary. For general ρ, the following equality holds:

$$\mathscr{I}_{ZK} = \mathscr{I}_B + \frac{z_+}{h}\,\Pi^+ - \frac{z_-}{h}\,\Pi^- - \int_{-\infty}^{+\infty} \int_{z_-}^{z_+} (\phi + \rho\lambda)_x \,\mathrm{d}z\,\mathrm{d}x. \tag{3.39}$$

For the class of solutions of the incompressible Euler equations generated by solutions of (3.29) we have, through (3.34),

$$\int_{-\infty}^{+\infty} \int_{z_-}^{z_+} \phi_{xt} \,\mathrm{d}z\,\mathrm{d}x = -hP_\Delta. \tag{3.40}$$

Deriving with respect to time equation (3.39) and using (3.40), we see again that $\mathscr{I}_{ZK}$ is conserved independently of field boundary values. This continues to hold for two-layer set-ups including the case of disconnected domains, provided suitable initial and boundary conditions are chosen for the Clebsch variable λ. Generalizations of these results to classes of incompressible, stratified Euler-fluid motion not governed by (3.29) seem less known and deserve to be investigated separately.

4. Discussion

Inspired by a close examination of the air–water limit of two-layer flows in a channel, we have isolated a class of new phenomena in the motion of stratified fluids interacting with rigid boundaries, and provided some tools for its mathematical modelling. This class consists of a selection mechanism for conservation laws rooted in the topological properties of density isolines for the initial density configuration of an incompressible Euler fluid. Specifically, even when the fluid system possesses symmetries, such as translation invariance, the connection properties of density isolines can make classical conservation laws associated with the symmetry fail. Depending on the topology of pycnoclines, this failure can be treated by considering the appropriate boundary terms. However, this is not always possible, e.g. when pycnoclines intersect both boundaries, and in general explicit expressions for the corresponding conservation laws ought to be derived from an appropriate variational formulation of the motion equations. Note that boundary terms similar to the ones we have introduced also emerged during the investigation of Hamiltonian symmetries and conservation laws in Benjamin (1986). However, in the present case the corresponding boundary integrals arise from the different mechanism of boundary-intersecting pycnoclines. This, in general, contributes to breaking the conservation laws of horizontal momentum and Casimirs which apply for constant ρ along the boundary.

The air–water system offers perhaps the most transparent illustration of these topological effects, as boundary terms arise naturally in this context. When both the air and water domains are connected and extend to infinity, a one-parameter family of conservation laws, formed by the horizontal momentum and boundary terms, exists. However, if only the water domain is connected while disconnecting the air domain, by water being in contact with the upper plate over some finite region, only one member of the family is selected as a conserved quantity. On the other hand, when the water region is finite and the air domain is disconnected, even this member of the family fails to be conserved in general. For this case, we have provided explicit formulae for the horizontal momentum time derivative for special choices

of initial data (with zero initial velocity). For the asymptotic limit of a perturbation of a box-like initial domain, we have discussed the case of step-like data which can in principle be studied experimentally. These results have been compared with direct numerical simulations for two fluids with the one corresponding to air having a density as small as 1/160 that of the lower fluid. As to the limit of air density approaching zero, we remark that there are theoretical subtleties associated with the limit of zero thickness of the connecting sliver (figure 1). As we have observed in the context of a long-wave model (Camassa *et al.* 2013, Appendix C), these limits do not commute, and give different results according to which order relation is used for these two small parameters.

Finally, we mention that the results we have derived may provide useful monitoring quantities for studies of air-domain disconnection in a sloshing tanks (Abrahamsen & Faltinsen 2011), or internal wave propagation with trapped cores (Carr, King & Dritschel 2012). Ongoing work in these directions will be reported in the future.

Acknowledgements

We thank M. Cooker, W. Craig, A. Russo and V. Zakharov for discussions and useful comments on different aspects of this work. Partial support by NSF grants DMS-0509423, DMS-1009750, RTG DMS-0943851 and CMG ARC-1025523, as well as by the MIUR Cofin2010-2011 project 2010JJ4KPA is acknowledged. R.C. and M.P. thank the Dipartimento di Matematica e Applicazioni of Università Milano-Bicocca for its hospitality. In addition, ETH Zurich and the Fields Institute (R.C.), and UNC's Carolina Center for Interdisciplinary Applied Mathematics (G.O.), are gratefully acknowledged for their hospitality while some of this work was being completed.

Appendix.

Using the results of § 2 it is possible to compute the value of pressure difference for a generic interface $\varepsilon L\beta(z)$ of small amplitude εL. For every interface that can be written as a Fourier series,

$$\beta(z) = \sum_{m=0}^{\infty} c_m \cos(m\pi z/h), \quad c_m = \frac{2}{h}\int_0^h \beta(z)\cos(m\pi z/h)\,\mathrm{d}z, \tag{A 1}$$

the pressure value K at the first asymptotic order in the limit $\varepsilon \to 0$ can be obtained by superposition due to linearity in β. We have

$$K \equiv K(\beta) = \sum_{m=0}^{\infty} c_m K^{(m)} + o(\varepsilon), \tag{A 2}$$

where $K^{(m)}$ is the value of the pressure when the interface β is the single Fourier mode $\cos(m\pi z/h)$. Setting $\beta(z) = \cos(m\pi z/h)$, with $m \geqslant 1$, formula (2.33) yields $K^{(m)} = o(\varepsilon)$ if m is even and

$$K^{(m)} = \frac{2}{m\pi}\rho_w g\varepsilon L \tanh\left(\frac{m\pi L}{2h}\right) + o(\varepsilon) \quad \text{if } m \text{ is odd.} \tag{A 3}$$

Using relation (A 2) yields

$$K(\beta) = \frac{2}{\pi}\rho_w g\varepsilon L \sum_{n=0}^{\infty} \frac{c_{2n+1}}{2n+1} \tanh\left(\frac{(2n+1)\pi L}{2h}\right) + o(\varepsilon). \tag{A 4}$$

Typically L is larger than h and therefore the hyperbolic tangent gives an exponentially small contribution which can be neglected for all n. For example, in the practically

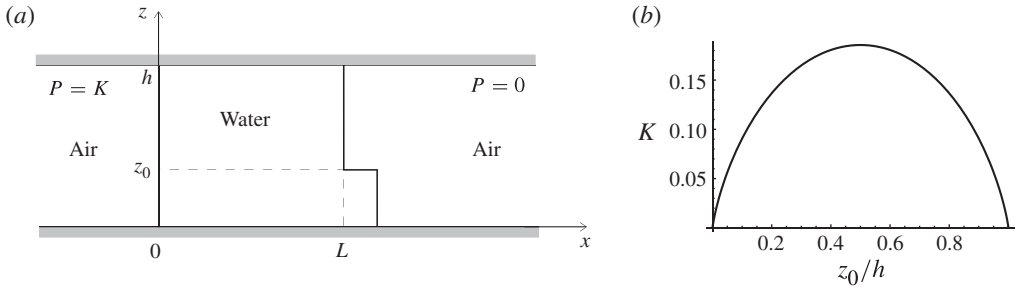

FIGURE 4. (*a*) A simple step-like initial configuration for the air–water system. (*b*) The corresponding value for the pressure difference K (A 6) versus height z_0 of the step, plotted with $\varepsilon = 0.1$, $L = 5h$ and $\rho_w = 1$, $g = 1$.

realizable step-like configuration $\beta(z) \equiv H(z_0 - z)$ (figure 4),

$$c_m = \frac{2}{m\pi} \sin(m\pi z_0/h), \quad m > 0. \tag{A 5}$$

Thus, to leading-order in ε the pressure difference for this step-like interface is

$$K(\beta) \sim \frac{4}{\pi^2} \rho_w g \varepsilon L \sum_{n=0}^{\infty} \frac{\sin((2n+1)\pi z_0/h)}{(2n+1)^2} = -\frac{2\rho_w g \varepsilon L}{\pi h} \int_0^{z_0} \log\left(\tan\left(\frac{\pi z}{2h}\right)\right) \mathrm{d}z. \tag{A 6}$$

REFERENCES

ABRAHAMSEN, B. C. & FALTINSEN, O. M. 2011 The effect of air leakage and heat exchange on the decay of entrapped air pocket slamming oscillations. *Phys. Fluids* **23**, 102107.

ALMGREN, A. S., BELL, J. B., COLELLA, P., HOWELL, L. H. & WELCOME, M. L. 1998 A conservative adaptive projection method for the variable density incompressible Navier–Stokes equations. *J. Comput. Phys.* **142**, 1–46.

BENJAMIN, T. B. 1968 Gravity currents and related phenomena. *J. Fluid Mech.* **31**, 209–248.

BENJAMIN, T. B. 1986 On the Boussinesq model for two-dimensional wave motions in heterogeneous fluids. *J. Fluid Mech.* **165**, 445–474.

BIDONE, G. 1820 Experiénces sur le remou et sur la propagation des ondes. *Mem. de l'Acad. Royale des Sciences de Turin, Tome XXV*.

CAMASSA, R., CHEN, S., FALQUI, G., ORTENZI, G. & PEDRONI, M. 2012 An inertia 'paradox' for incompressible stratified Euler fluids. *J. Fluid Mech.* **695**, 330–340.

CAMASSA, R., CHEN, S., FALQUI, G., ORTENZI, G. & PEDRONI, M. 2013 Effects of inertia and stratification in incompressible ideal fluids: pressure imbalances by rigid confinement. *J. Fluid Mech.* **726**, 404–438.

CARR, M., KING, S. E. & DRITSCHEL, D. G. 2012 Instability in internal solitary waves with trapped cores. *Phys. Fluids* **24**, 016601.

CRAIG, W. & SULEM, C. 1993 Numerical simulation of gravity waves. *J. Comput. Phys.* **108**, 73–83.

HOWARD, L. N. & YU, J. 2007 Normal modes of a rectangular tank with corrugated bottom. *J. Fluid Mech.* **593**, 209–234.

LANDAU, L. D. & LIFSHITZ, E. M. 1987 *Fluid Mechanics*. Pergamon.

MORRISON, P. J. 1998 Hamiltonian description of the ideal fluid. *Rev. Mod. Phys.* **70**, 467–521.

VANDEN-BROECK, J.-M. & KELLER, J. B. 1989 Pouring flows with separation. *Phys. Fluids* A **1**, 156–158.

ZAKHAROV, V. E. & KUZNETSOV, E. A. 1997 Hamiltonian formalism for nonlinear waves. *Phys. Usp.* **40**, 1087–1116.

ZAKHAROV, V. E., MUSHER, S. L. & RUBENCHIK, A. M. 1985 Hamiltonian approach to the description of nonlinear plasma phenomena. *Phys. Rep.* **129**, 285–366.